Design of a counter rotating fan using a multidisciplinary and multifidelity optimisation under high level of restrictions

Lionel Meillard
lionel.meillard@dlr.de
DLR, German Aerospace Center
Fan and Compressor Department
Cologne
Germany

Cristian Mihail Stanica
COMOTI, Romanian Research and
Development Institute for Gas Turbines
Stress and Vibration Analysis Department
Bucharest
Romania

Nabil Ben Nasr
ONERA, The French Aerospace Lab
Aerodynamic, Acoustic and Aeroelasticity
Department
Meudon
France

William Riéra
Safran Aircraft Engines
Low Pressure Compressor R&T Department
Moissy-Cramayel
France

ABSTRACT

A model scale ducted counter-rotating fan was designed by DLR, ONERA, COMOTI and Safran Aircraft Engines within the frame of the EU-project COBRA, (Europe-Russia cooperation within FP7 program coordinated by ONERA for the European side and CIAM for the Russian side). The design was very challenging due to the multidisciplinary aspects of the problem and the high number of very restrictive constraints.

This work is based on the previous EU-project VITAL (within FP6 program), objectives of which have been motivated by the ACARE-goals, namely reducing noise by 10 dB, NO_x by 60% and the specific fuel consumption by 20%. The COBRA project investigated further different technical solutions to overcome the insufficient noise performance of the VITAL CRTF. An acoustic level reduction by 3 dB for all acoustic operating points has been defined as target compared to the best VITAL CRTF. To achieve these goals, a higher bypass ratio is explored resulting in much lower blade tip speeds and blade count while maintaining good aerodynamic performances.

The multidisciplinary approach and the numerical tools used are described. The final CRTF geometry is based on a multiobjective and multifidelity optimisation method and derived from an initial geometry (V0) provided by Safran Aircraft Engines. During the optimisation process, all created members are evaluated with 3D RANS calculations for the CRTF aerodynamics performance, and FEM calculations for the blade structural properties. A simple acoustic evaluation provided by ONERA using steady calculation results allows to estimate the CRTF acoustic level at approach condition.

The number of blades chosen fixed during the optimisation is 11 blades for the front fan and 8 for the rear fan. More than 100 free parameters are used to characterize one blade geometry, which is defined by five profiles evenly distributed in the spanwise direction.

The final geometry (V4) of the counter-rotating fan achieves an efficiency similar to the previous VITAL CRTF at design point but reduces the noise of -3 dB at approach operating point, while satisfying the mechanical constraint of titanium and maintaining a very strict range of torque ratio as well as a very low residual swirl. Concerning this last point, the multifidelity optimisation method has been very helpful to respond the high level of requirements.

Keywords: Counter rotating fan; multidisciplinary; multifidelity; optimisation; 3D design; tonal noise

NOMENCLATURE

ACARE	Advisory Council for Aerodynamics Research in Europe
ADP	Aerodynamic Design Point (OP0)
BPR	ByPass Ratio
CAA	Computational Aero Acoustics
CFD	Computational Fluid Dynamics
COBRA	Contra rOtating fan system for high Bypass Ratio Aircraft engine
CRTF	Counter Rotating Turbo Fan
elsA	Ensemble logiciel de simulation en Aérodynamique
FEM	Finite Element Method
ISA	International Standard Atmosphere
NASTRAN	NAsa STRuctural ANalysis
OAPWL	OverAll sound PoWer Level
OP	Operating Point
OGV	Outlet Guide Vane
RANS	Reynolds-Averaged Navier-Stokes
RPM	Revolutions Per Minute
TRACE	Turbomachinery Research Aerodynamics Computational Environment
TR	Torque Ratio
UHBR	Ultra-High Bypass-Ratio
VITAL	EnVIronmenTALly Friendly Aero Engine

Symbols

α	Fan 2 sweep angle at leading edge in tip region
$\dot{m}$	Mass flow rate
S	Section surface defined by fan 1 leading edge
ω_1, ω_2	Fan rotational speeds
d	Axial distance between the two fans
c_x	Axial chord
T_t	Total temperature
V_x	Axial velocity

1.0 INTRODUCTION

1.1 Project objectives

COBRA is a 3.5-year FP7 collaborative research project between Europe and Russia (under grant agreement No 605379), started in October 2013. Coordinated by ONERA, it associates 9 European partners. The philosophy of COBRA is to use the complementarity of EU-Russian expertise in ducted architectures to assess, at the whole engine level, the capabilities of the Ultra High Bypass Ratio (UHBR) Contra Rotating TurboFan (CRTF) in terms of performance and acoustic levels.

In the past, CRTF architectures were already studied. On European side, the definition of several CRTF designs, with Bypass Ratio (BPR) of 10-11, were achieved in the scope of the VITAL project and tested at CIAM C3-A test rig facility [1] [2]. It was concluded that CRTF approach offers a good alternative to the classic turbofan regarding the performance. However the acoustic level of this concept was not improved, when compared to the year 2000 baseline single fan at the same bypass ratio. On Russian side, the UHBR CRTF has already been studied and is developed since 1990 by Kuznetsov for use on small-medium range aircraft. The NK-93 gearbox turbofan engine has been designed with a bypass ratio of 16.5 and tested in flight condition in 2007. This engine has been designed 20 years ago under old constraints in terms of environmental targets.

Based on this past experience and on the actual design tools, the implementation of CRTF architecture to the UHBR approach is studied in order to overcome the insufficient noise performance of the counter-rotating fan tested in the VITAL project. Higher bypass ratio designs with much lower blade tip speeds and blade counts will be explored, whilst at least maintaining and maybe increasing the good aerodynamic efficiency already achieved during the VITAL project. Starting from specifications and baseline geometry (V0), defined by Safran Aircraft Engines, ONERA and DLR performed multidisciplinary design activities in order to propose a CRTF module design (V4) to be manufactured by COMOTI and tested by CIAM.

1.2 From high level specifications to a preliminary design

The first step in the Safran Aircraft Engines design process for COBRA was to define the target concerning the aircraft platform. A short/medium range aircraft has been chosen to keep consistency with other EU projects, therefore, the DREAM (open rotors) aircraft platform is used as target to design the COBRA CRTF engine [3]. A thermodynamic cycle optimisation is conducted to spot the most relevant engine architecture configuration, considering different gearbox architectures.

An important aspect of CRTF engines is the possibility to avoid using Outlet Guide Vane (OGV) in the secondary flowpath. A configuration with no OGV is more complex to design to reach an axial exit flow. This implies that the torque ratio between fans must be close to unity at every operating condition. A constant torque ratio is possible only with the use of a differential gearbox to drive the fan rotors from a single Low Pressure (LP) turbine. Different cycle versions are provided to the Low Pressure Compressor (LPC) design team. These 0D data are used to design the duct and 1D blade models. Various parameters are evaluated with Safran Aircraft Engine´s throughflow in-house code. Several values of BPR, specific flow, speed ratios between the two fans and blade count were studied as well. The final choice with a BPR of 16 is then a compromise between aerodynamic and acoustic goals, taking into account weight and integration constraints.

Once converged on an optimum cycle version, the 3D blades are designed and then evaluated by the CFD solver *elsA*. Different 3D blade geometries are tested before reaching the required aerodynamic and mechanical performance for the different operating points. The last version, known as V0, is then sent to COBRA EU partners with low level (CRTF module related) specifications so that they can carry on the optimisation.

1.3 Defining constraints for the Multidisciplinary optimisation

The low level specifications are based on the high level requirements and the feasibility study done during the design process which has led to the V0 version.

The flow capacity and global fan pressure ratio at aerodynamic design point (ADP), also called OP0, are constraints needed to achieve high propulsive efficiency through high BPR choice. The torque ratio is imposed by the differential gearbox layout and cannot be changed during the optimisation process. In addition, the engine operation requires for the CR fan module a sufficient stall margin (last numerical converged point called OP1) and flutter margin, which are given as specifications. In order to ensure optimum propulsive efficiency from the bypass channel, a maximum residual swirl is specified too. Finally, a range of acceptable speed ratios and average reduced speeds is defined for ADP.

Concerning the blade count, the constraint is linked to aerodynamic feasibility, acoustic constraints and cost specifications. The blade geometry variations are mainly limited by:

- Mechanical constraints: aspect ratio, leading edge and trailing edge thicknesses, so that the blades can withstand Foreign Objects Damages.
- Acoustic constraints for approach condition (point called OP2): minimum fans axial spacing defined by (d/cx) at 10% and 90% blade height, minimum sweep angle (α) value for the second fan.

All these challenging specifications are set so that the counter rotating fan design is representative of a modern UHBR engine.

2.0 DESIGN METHODOLODY

2.1 Multifidelity Design Optimisation

2.1.1 Optimiser setup

Optimisation algorithms are very important tools in the process of turbomachinery design. The past few years have shown that optimisation algorithms have become more complex, reaching a high maturity level of performing more complex multidisciplinary and multiobjective design. However this tendency leads to an increase in the number of design variables, impacting the optimisation time required to solve a problem.

The optimisation is based on an evolutionary algorithm parallelised in an asynchronous manner using a master-slave communication [4] [5]. A new feature of the DLR-in-house optimiser AutoOpti has been developed and tested during the COBRA project: the multifidelity optimisation [6] [7]. Figure 1 represents the general AutoOpti structure. Multifidelity is a way to reduce the required time to train the metamodel by using two different levels of accuracy, called low and high fidelity process chain. A newly generated member can be evaluated either by the low or the high fidelity process chain. The low fidelity process chain allows calculating members quickly (about 7 times faster than the high fidelity process chain in this case) to enlarge the database on which the metamodel is based. In the low fidelity process chain, the level of accuracy of the CFD and FEM calculations is lowered by reducing the resolution of the domain discretisation (see section 2.2.1 and 2.3).

A decision function has been defined in order to impose the ratio between the number of members calculated with the high and the low fidelity process chain during the optimisation. This function is a decreasing linear function starting at 80% low fidelity members. By this way a very high amount of low fidelity members is calculated, at the beginning of the optimisation. Moreover 30 stochastically generated members are calculated to start the optimisation.

The process chain of the optimisation is depicted in Figure 1 on the right side. The methodology dedicated to CFD, FEM and acoustic calculations will be described in the following subsections.

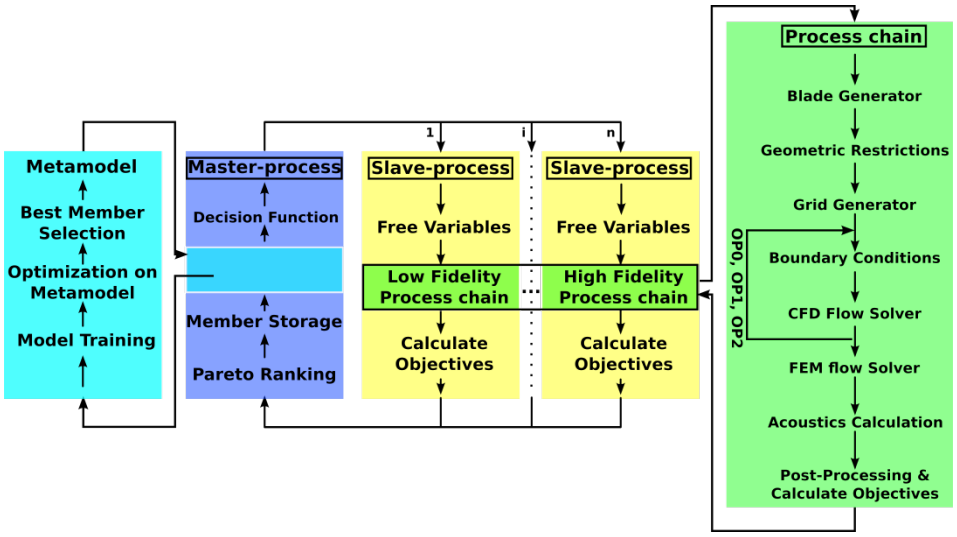

Figure 1 AutoOpti multifidelity flow-chart

2.1.2 Objective functions and restrictions

A high priority has been given to the isentropic efficiency and the acoustic of the COBRA counter rotating fans design. The goal was to maintain at least the efficiency reached by the previous CRTF from VITAL and at the same time to improve the tonal noise emitted by the COBRA CRTF at approach condition. Two objective functions have been defined for the optimisation: the isentropic efficiency of both fans at design point and the integrated tonal sound pressure level spreading in the downstream direction at approach condition.

Because of the multidisciplinary aspect of this design, the number of restrictions is high. 15 restrictions are considered concerning different aspects of the design: geometric, aerodynamic, mechanic and acoustic. The given restrictions were set in narrow margins. Moreover, all the restrictions were not fulfilled by the initial geometry V0 according to the DLR methods used during the design process. Table 1 and Figure 2 give the definitions of the objectives and the main restrictions, their corresponding tolerance margin as well as an indication of their fulfilment by V0.

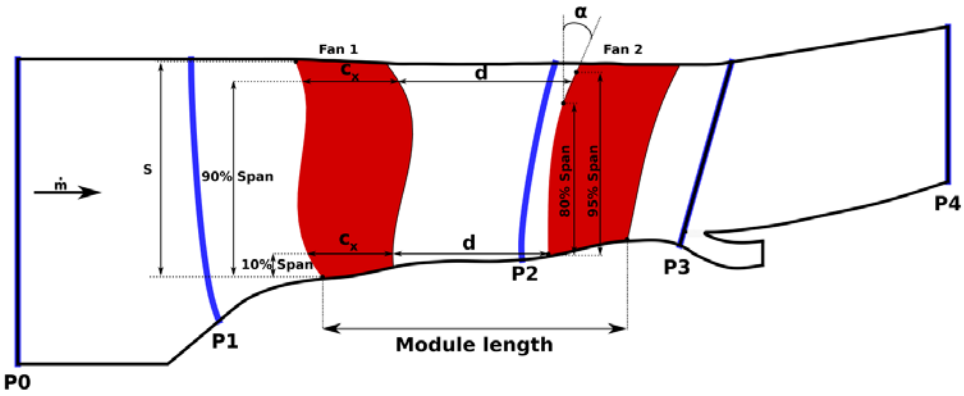

Figure 2 Main geometrical restrictions of the blades (initial geometry V0 in red) and position of the stations for aerodynamic calculation

Table 1 Definition of objectives and main restrictions used during the design process

	Name	Unit	Operating Point	Definition	Margin	Fulfilled by V0 (DLR methods)
Objectives	**Isentropic efficiency**	[-]	OP0	Isentropic efficiency calculated between the station P1 and P4	To maximize	
	Integrated sound pressure level	[dB]	OP2	Integrated sound pressure level emitted in the downstream direction calculated with a criterion (see section 2.4.1)	To minimize	
Aerodynamic Restrictions	**Flow capacity**	[kg/s/m^2]	OP0	Ratio of the mass flow ($\dot{m}$) entering the compressor at P1 and the section surface (S) defined by the front fan leading edge: $\frac{\dot{m}}{S}$	±0.5%	Yes
	Global total pressure ratio	[-]	OP0	Total pressure ratio calculated between the station P1 and P4	±0.7%	No with DLR methods
	Stall margin	[%]	OP0/OP1	Distance (SM) between the ADP operating point (OP0) and the last converged point near stall margin (OP1) at 100% RPM on the performance map (see Figure 6)	>10%	No with DLR methods
	Residual swirl angle	[°]	OP0	Mass averaged flow angle leaving the rear fan	<baseline	No
	Torque ratio	[-]	OP0	Torque ratio (TR) calculation based on the total temperature ratio at station P1, P2 and P3: $\frac{T_{t3}-T_{t2}}{T_{t2}-T_{t1}}\frac{\omega_1}{\omega_2}$	±2%	No with DLR methods
Mechanic Restrictions	**Von-Mises stresses**	[MPa]	OP0	The Von-Mises stresses distribution of the blades has been calculated using CalculiX (see section 2.3.1)	n.c.	No
	Flutter	-	OP0	Flutter criterion based on flexion and torsion modes of the blades are used in order to avoid flutter at ADP	n.c.	n.c.
	Structure and fan dynamic	-	-	Calculation of the Campbell- Diagram. A list of resonance crossing has been defined in order to avoid any unacceptable vibrations amplitude on the fan blades	>5% in rotation speed	No
Geometric Restrictions	**Axial distance to chord**	[-]	-	Ratio between the fan axial distance (d) and the fan 1 axial chord (c_x) at 10% span of fan 1	n.c.	Yes
				Ratio between the fan axial distance (d) and the fan 1 axial chord (c_x) at 90% span of fan 1	n.c.	Yes
	Fan 2 sweep angle	[°]		Angle (α) between the vertical and the line passing the leading edge points located at 80% and 95% span of fan 2	n.c.	No

2.1.3 Free parameters and parameterisation

The free parameters are dominated by the parameterisations of each blade geometry. The tool used for the blade generation is the DLR-in-house tool Bladegenerator, already used in the scope of counter rotating fan design [8]. 3D blade geometry is defined by 5 profiles at different spanwise positions in red and green on Figure 3 (top). Each profile is created by geometric design parameters depicted on Figure 3 (bottom). The orientation of the profile is given by the leading (β_{LE}) and trailing edge angle (β_{TE}) as well as the stagger angle (β_{ST}). The point PT_1 and PT_2 (blue stars) allow the construction of the suction side spline. Then the pressure side is deduced from a thickness function distribution with the parameter (D_{max} and D_{maxx}). Before the stacking of the blade, the lean (X_{LE} and X_{TE}) and the sweep (θ) are controlled allowing placing each profile in the axial and the meridional directions. The sum of all different free parameter leads to 112 design parameters.

The number of blades for each fan are chosen constant namely, 11 for the front fan and 8 for the rear fan. The rotational speeds for both fans are defined as free parameters and a degree of freedom of +/-1% of the specified rotational speed at design point is given.

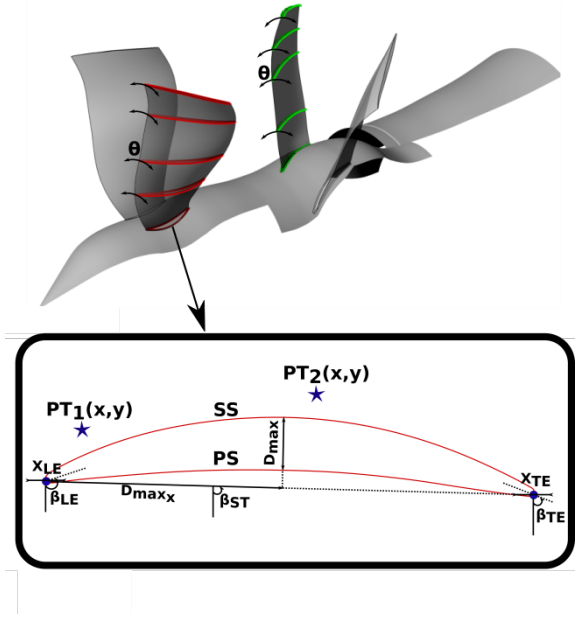

Figure 3 Example of profile's stacking (top) and the parameterisation for one profile (bottom)

2.2 CFD calculations

The computational domain taking into account the bypass region behind the rear fan is depicted in Figure 3. Low and high fidelity meshes are used during the multifidelity design process. A comparison between both meridional meshes is depicted in Figure 4. Attention has been paid in order to choose a low fidelity grid allowing the lowest computational time while keeping sufficient confidence in the CFD results. In contrast, the high fidelity mesh is representative of a standard mesh dedicated to turbomachinery applications. Both meshes are based on an OCH topology of structured blocks. Two mixing planes are used: one between the fans and another between the rear fan and the bypass region. The low Reynolds and wall function approaches are applied to the high and the low fidelity mesh respectively. The grid´s properties as well as the calculation times needed for one run are given in Table 2.

Table 2 Low and high fidelity CFD mesh properties

	Total Cell Number	Radial discretisation	Y+	Calculation Time (relative)
Low Fidelity	300.000	21	Wall function	1/4
High Fidelity	2.000.000	69	Low Reynolds	1

The simulations are carried out using the solver TRACE [9] [10] developed at the DLR Institute of Propulsion Technology. All calculated members during the optimisation are achieved by solving the steady-state Reynolds-Averaged Navier-Stokes (RANS) equations in a single blade passage at rig scale. Turbulence is modeled by the k-ω Wilcox model. Total pressure, total temperature and flow angle are specified uniformly at the inlet boundary following the International Standard Atmosphere (ISA) conditions. Viscous-wall and adiabatic conditions are imposed on all solid walls.

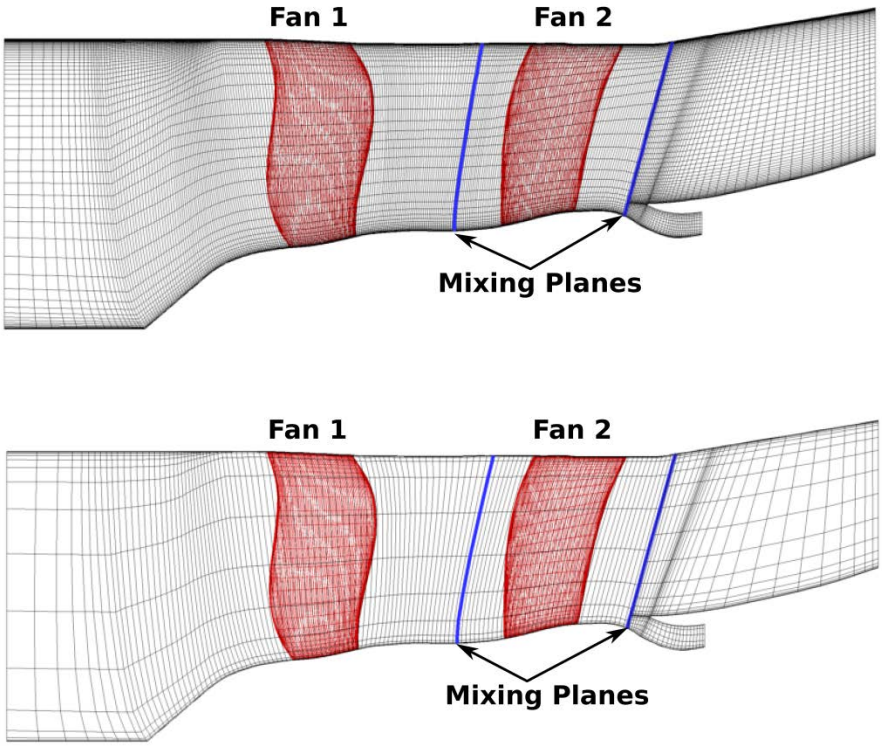

Figure 4 High (top) and low fidelity (bottom) meridional grid showing the positions of the V0 fans

2.3 FEM calculations

2.3.1 FEM calculations with CalculiX for optimisation process

The FEM solver CalculiX [11] is integrated in both process chains to estimate the Von Mises stresses, the radial deformation and the Campbell-Diagram of the blades (hot). Those calculations are based on the quadratic finite element method and the static pressure distribution on the blade from the CFD solution. It should be mentioned, that the model used is very simple as only the wetted part of the blade is taken into account during the calculations. As in CFD calculations, also for FEM, two meshes have been used for the multifidelity optimisation. The Table 3 compares both FEM setups.

2.3.2 FEM calculations with NASTRAN for validation

One important aspect of design effort was to ensure that the low and high fidelity models used during the optimisation process are close to reality. For this reason, a very fine FEM model has been punctually performed by COMOTI for each major optimisation iteration in order to validate the results of CalculiX. A structured grid was developed modeling the blade itself. The blade foot and details of the fillet region are also taken into account unlike in the CalculiX calculations. The structure mesh containing hexahedron elements assures the maximum precision of the results. The software chosen to perform the stress and vibration analysis is NASTRAN (NAsa STRuctural ANalysis). Because of the chosen architecture for the COBRA CRTF, the material chosen for the blades was titanium alloy BT6 (TA6V) as for the CalculiX calculations. For the accurate stress and vibration analyses, the cold geometry domain has been chosen in order to take into account the stress stiffening of the blade when

deforming from the manufacturing (Cold) geometry to the operation (Hot) running geometry. In order to achieve this, a Hot to Cold transformation was performed. The Table 3 compares the NASTRAN FEM setup with the CalculiX setups.

Table 3 Low and high fidelity CalculiX FEM mesh properties compared to NASTRAN model

	Geometry	Model	Element	Cells Numbers	Calculation Time (relative)
CalculiX - Low Fidelity	Hot	Only blade	Quadratic	2376	1/3
CalculiX - High Fidelity	Hot	Only blade	Quadratic	19000	1
NASTRAN	Cold	Blade with Fillet and foot	Hexahedron	138794	3

2.4 Acoustic calculations

2.4.1 Acoustic evaluation with ONERA criterion

The method integrated in the optimisation process and proposed by ONERA is based on the use of Amiet's theory [12] [13], which is already used for aeroacoustics design of classic turbofans. It is combined with Hanson's theory developed for the open fans [14] and adapted here to ducted fans. This approach requires many simplifications related to the flow and to the geometry. The main assumptions are the following:

- The source generation is only due to the impacts between the upstream fan wakes interacting with the downstream fan.
- The blades are modelled by untwisted and non-cambered flat plates as in the Amiet theory devoted to isolated airfoils.
- The duct propagation is accounted for assuming fully annular geometry and a uniform axial mean flow in order to describe the sound field as Fourier-Bessel modes.
- The flat plate chord is assumed to be aligned with the convection flow which determines the value of the stagger angle.

However, despite of these raw assumptions discussed here, the method is not limited to a pure aerodynamic criterion as the intensity or the momentum value of the wake velocity defects [15], but is directly related to integrated sound pressure level or overall sound power level (OAPWL) which is used as an objective function in the optimisation process. Only the sound pressure level emitted from the rear fan in the downstream direction is considered as objective function. The inputs to the Amiet-based formulation are the wake characteristics behind the downstream fan that are provided by the steady RANS at OP2 calculation. An S3 surface has been extracted upstream the mixing plane. Then the CFD data corresponding to the three components of the velocity are interpolated on a uniform grid. The data are provided in the absolute frame over a cross-section covering a single first fan blade channel.

2.4.2 Computational Aero Acoustic calculations (CAA) for validation

In addition to acoustic evaluation performed with acoustic criterion by ONERA and Safran Aircraft Engines, unsteady CFD computations were performed in order to perform CAA analysis and to have a better confidence in the V4 acoustic performance as shown in Figure 9. These computations were conducted by using a structured grid adapted to the acoustic purposes. The main characteristics of the grid used are: 18 million cells, 221 points in span direction, 185 points around each profile and 97 points in azimuthal direction. The flow is discretised on a single blade-passage per blade-row, using chorochronic periodicity conditions [16] (phase-lag) for the cylindrical cases. This approach provides great reductions in CPU time compared to the full annulus approach. Unsteady Reynolds-Averaged Navier-Stokes equations are solved by ONERA-in-house CFD code *elsA* [17]. Time discretisation is implicit based on Runge-Kutta (RK4)

approach with local time stepping. Time integration is based on O(Δ2) backward Euler approach with Implicit scalar LUrelax. Space discretisation uses the 2nd order Jameson cell-centered scheme with artificial dissipation. The Jameson artificial viscosity values are set to the values κ2=0.5 and κ4=0.016. Based on previous experience with open rotors and turbofans, the k-ε turbulence model is chosen. Steady computations were performed first in order to be used as initialisation for unsteady computations. After convergence the unsteady wall pressure distribution is used for CAA analysis.

3.0 RESULTS OF THE MULTIFIDELITY OPTIMISATION

3.1 Aerodynamic Results

The final geometry V4 is depicted (in green) and compared with the initial geometry V0 (in red) in Figure 5. An increase of 16% in module length is observable. The value of the main geometrical restrictions and a comparison between V0 and V4 are given in Table 4. The general rear fan shape has been significantly modified in order to reach the geometric, acoustic and the mechanic restrictions.

Table 4 Low and high fidelity CFD mesh properties

	V0	**V4 compared to V0**
Module length	baseline	+16%
d/c_x **at 90%**	baseline	+17%
d/c_x **at 10%**	baseline	+9%
α	baseline	+24%

The global high fidelity aerodynamics performances at 100% RPM of both geometries are depicted in Figure 6. The operating points OP0 and OP1 are circled in red for V0 and V4. At OP0, the flow capacity changed only slightly between both geometries. The total pressure ratio restriction is fulfilled by V4 with a decrease of -0.036. The torque ratio (TR) was very challenging to fulfil while keeping at the same time a minimal residual swirl. The freedom of liberty given to the fan rotational speeds allowed to reach this target. The optimised geometry reached an improvement of +2% in efficiency which was defined as an objective function all along the optimisation process. The stall margin (SM) with OP1 has been also improved with the new geometry V4 and fulfilled the restriction (SM >10%) according to the DLR methods.

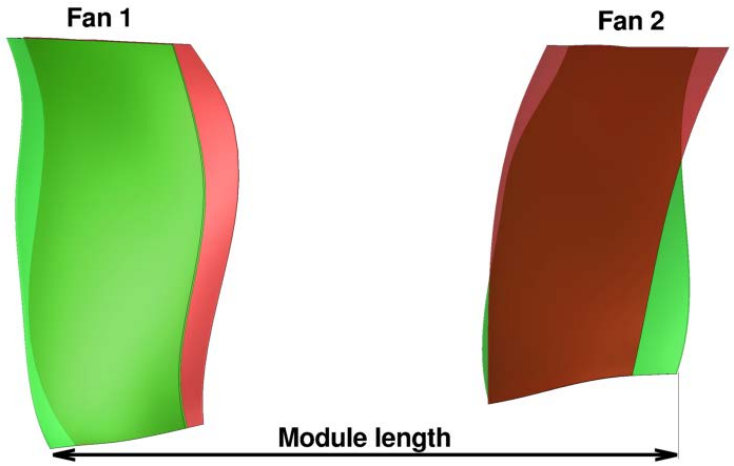

Figure 5 The initial 3D geometry V0 in red and the optimised 3D geometry V4 in green

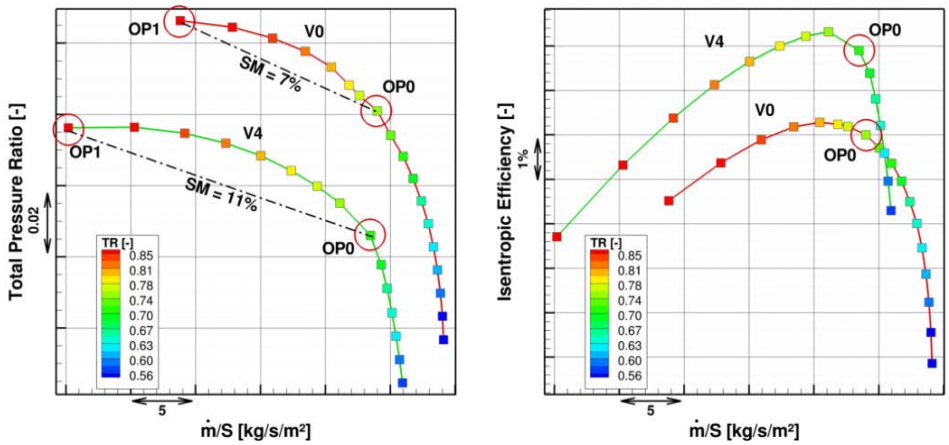

Figure 6 Performance Map of initial (in red) and optimised (in green) geometry at 100% RPM with evolution of torque ratio along the speedline

The isentropic Mach number distribution on the suction side of the blade is depicted in Figure 7 for both geometries as well as for the low and the high fidelity mesh. For a given geometry, the same structures are observed with both meshes: the positions as well as the intensity of the shock are well described in both meshes. A significant difference can be nevertheless observed for the geometry V4 at the rear fan. Indeed, the low fidelity mesh shows the presence of a strong shock all along the span near trailing edge whereas the high fidelity mesh shows the presence of a second shock region directly located at the leading edge. Between V0 and V4, the shock intensity of fan 1 has been reduced in the tip region with the loss of the expansion shock but has been increased in the hub region. The strong passage shock on the V0 rear fan has been transformed into two weak shocks on the upper part of the blade. These are also visible on the meridional view in Figure 7.

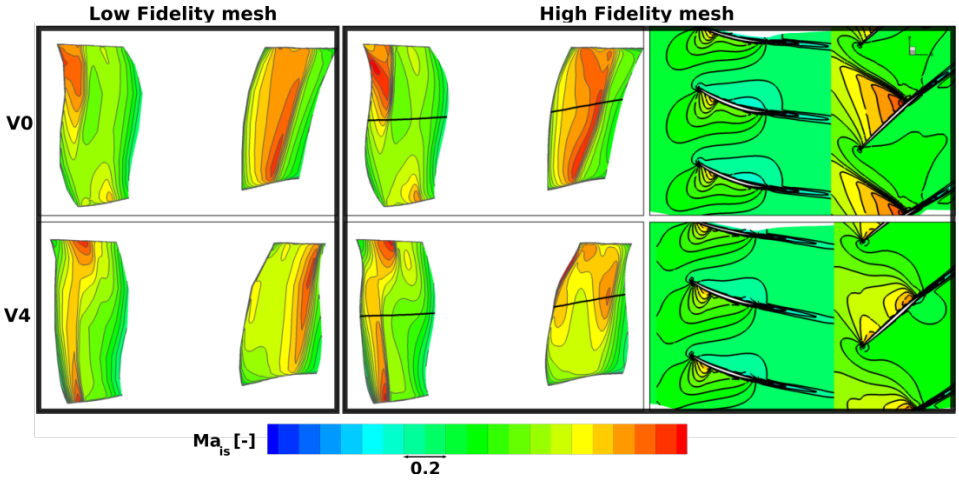

Figure 7 Isentropic Mach number distribution on blade suction sides and at mid span in a meridional view for high fidelity mesh

3.2 Acoustic Results

It is important to remember that only the approach operating point is taken into account for the acoustic objective function. The other interesting acoustic points, cutback and sideline, have been calculated additionally with the ONERA criterion and CAA calculations. All the results are depicted in Figure 8. A significant acoustic improvement by about 7 dB is visible between V0 and V4 for all acoustic operating points. When the low fidelity mesh is considered, this noise reduction is also visible but the improvement is a bit less compared to the decrease calculated with a high fidelity mesh (about 3 dB). The low fidelity resolution seems to be enough to capture those acoustic improvements. The CAA calculations were carried out only for the V4 geometry and the results match well with those from the ONERA criterion. Regarding

the previous VITAL CRTF, the V4 geometry shows an acoustic reduction of about 3 dB reaching by this way the COBRA objective.

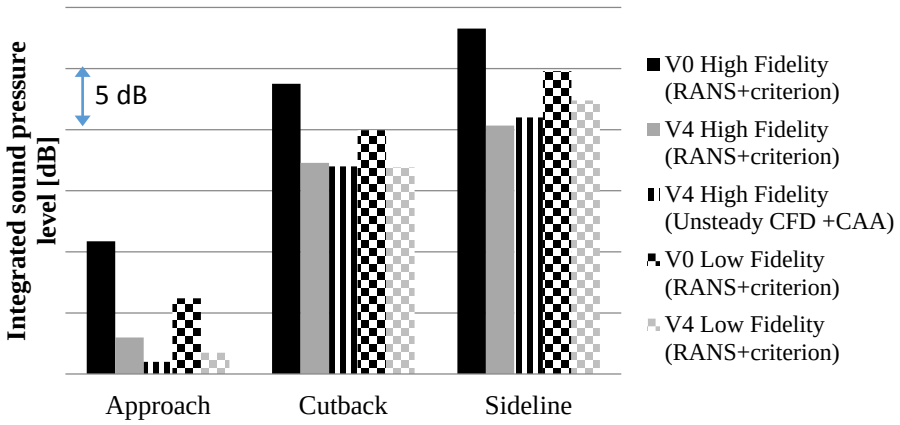

Figure 8 Integrated sound pressure level emitted in the downstream direction: Comparison between V0 and V4 at approach, cutback and sideline

The improvement of the acoustic levels shown in Figure 8 is not due to the modification of the rear fan shape since the acoustic criteria considers the rear fan as a flat blade as explained in section 2.4.1. So it appears that the improvement is the result of positive modification of the wakes behind the front fan. Figure 9 represents the wake axial velocity extracted from the high fidelity mesh for V0 (left) and V4 (right). The grid depicted in Figure 9 is the interpolation grid used as input for the acoustic criterion. The impact of the wake has been reduced in the upper part.

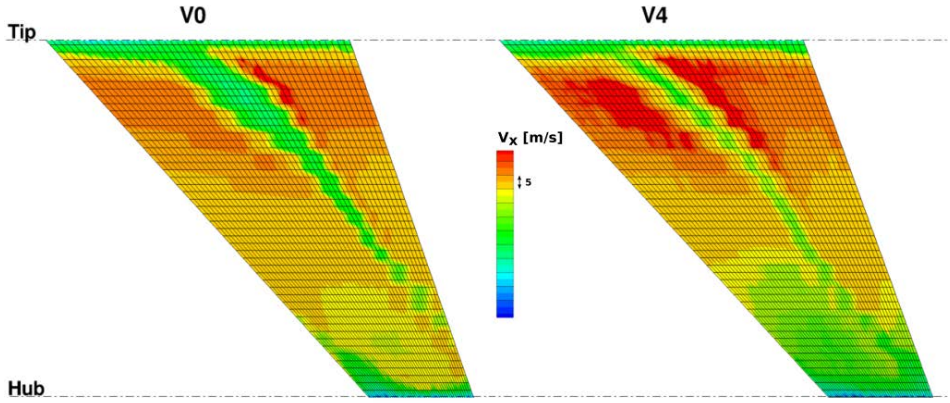

Figure 9 Wake comparison at approach for V0 (left) and V4 (right) data extracted from the high fidelity mesh extracted before the mixing plane

3.3 FEM Results

Figure 10 shows the improvement of the Von Mises distribution on the fan 2 suction side between V0 and V4 in different FEM models. The CalculiX low and high fidelity models considering only the wetted part of the blade give results which are very close together. Indeed, the same stresses levels and distribution are visible. It is shown that the V0 geometry does not fulfil the Von Mises specification because two significant stress spots are visible. The Von Mises stresses of the optimised geometry V4 has been reduced everywhere expected, very locally, at the trailing edge in the hub region. In this region a high Von Mises stress spot is located. It should mentioned that this region was not taken into account in the optimisation process as the Von Mises stresses depend to a large part on the foot and the fillet geometry. The NASTRAN model shows also a good improvement regarding the maximum Von Mises stress. As shown in Figure 11, the V4 geometry presents a reduction of 62% in stress for the rear blade compared to the initial

V0 cold geometry. The presence of the fillet and the foot decreases the stress located in the hub part below the specification value with a sufficient margin.

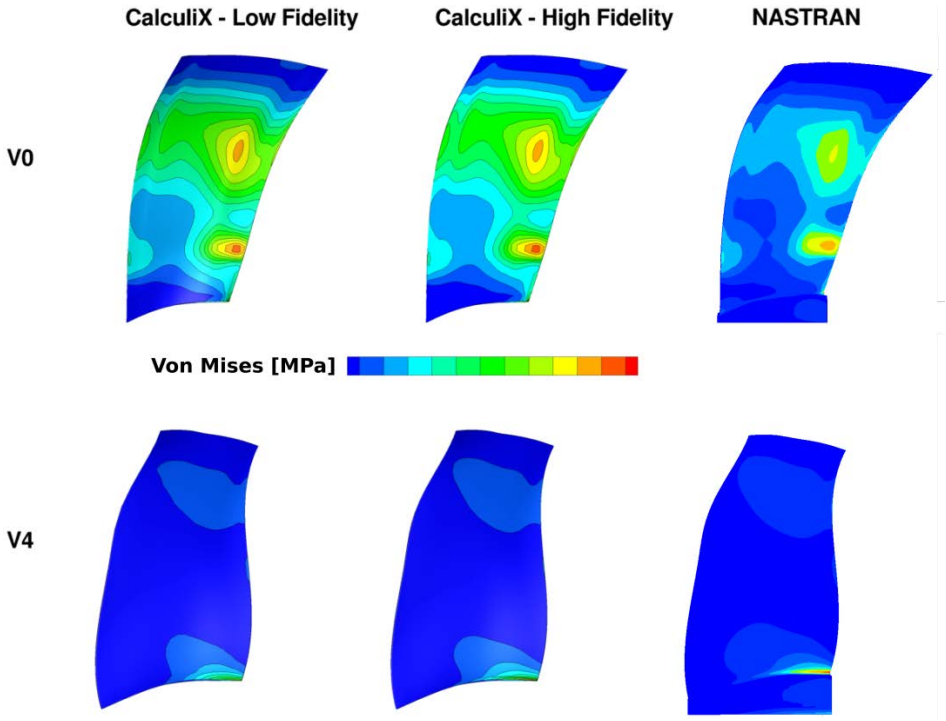

Figure 10 Von Mises distribution on fan 2 blade suction side comparison between V0 and V4 for different models

4.0 CONCLUSION AND OUTLOOKS

A set of specifications representative of a modern UHBR CRTF (BPR=16) engine and an initial geometry V0 have been defined by Safran Aircraft Engines. The design process using a multidisciplinary and a multifidelity optimisation was carried out in cooperation with ONERA, COMOTI and Safran Aircraft Engines. A complete optimisation has been conducted taking into account the aerodynamic, mechanic and acoustic aspects. Two objectives functions were implemented in order to maximize the isentropic efficiency at the aerodynamic design point ADP and to reduce engine noise emission of COBRA by using the ONERA acoustic criterion. According to the DLR methods, not all the given specifications were fulfilled by V0 which made the design challenging. Moreover, it was difficult to maintain a very low residual swirl under the very strict torque ratio specifications. In that sense, the use of the multifidelity optimisation was helpful to reach the goals.

The obtained final geometry COBRA V4 fulfilled all the restrictions, maintained the level of efficiency previously reached by VITAL and reached an improvement of 3 dB at approach. The acoustic performance and mechanical constraints of V4 have been calculated by using CAA calculations and a very fine FEM model; by this way more confidence has been given to the results of the multifidelity optimisation. The manufacturing process of COBRA V4 is currently in progress at COMOTI and the CRTF will be tested during an experimental campaign before the end of 2017 in Moscow at CIAM C3-A, allowing cross comparisons with the numerical simulations.

ACKNOWLEDGMENTS

The authors would like to acknowledge François Julienne, Jérôme Talbotec and Nicolas Tantot from Safran Aircraft Engines for their supports all along the COBRA project. Further thank goes to Cyril Polacsek and Gabriel Reboul from ONERA for their help with the integration of the acoustic criterion in the design process. The authors are particularly grateful to their DLR´s colleagues Andreas Schmitz and Christian Voß for their assistance during the multifidelity optimisation, as well as to Rainer Schnell, the leader of the conception and design work package. A special thank goes to our CIAM partners for fruitful discussions and their continuous support.

REFERENCES

[1] Khaletskiy, Y., Mileshin, V., Talbotec, J., Nicke, E. "Study on Noise of Counter Rotating Fan Models at CIAM Anechoic Chamber." *ICAS*, 2012.
[2] Talbotec J., Vernet M. "Snecma counter rotating fan aerodynamic design logic & test results." *ICAS*, 2010.
[3] Tantot N., Julliard J. "From turbojet to innovative architectures: open rotor and contra rotative fan engines." *VKI lecture*, 2008.
[4] Aulich, M., and Siller, U. "High-Dimensional Constrained Multiobjective Optimization of a Fan Stage." 2011: No. GT201145618.
[5] Voss, C., Aulich, M., and Kaplan, B. "Automated Multiobjective Optimisation in Axial Compressor Blade Design." 2006: No. GT2006-90420.
[6] Kennedy, M., and O'Hagan, A. "Predicting the output from a complex computer code when fast approximation are available." 2000, Vol. 87 ed.: 1-13.
[7] Reimer, E. "Vergleichende Optimierung eines Fans mit High- und Multifidelity verfahren." Bachelor Thesis, Fachhochschule Aachen, 2016, 107.
[8] Lengyel, T., Voss, C., Schmidt, T., Nicke, E. "Design of a counter rotating fan-An aircraft engine technology to reduce noise and CO2-emissions." *ISABE*, 2009.
[9] Becker, K., Heitkamp, K., and Kügeler, E. "Recent progress in a hybrid-grid CFD solver for turbomachinery flows." *V European Conference on Computational Fluid Dynamics.* Lisbon, Portugal, 2010.
[10] Kügeler, E., Nürnberger, E., Weber, A., and Engel, K. "Influence of blade fillets on the performance of a 15 stage gas turbine compressor." *Proccedings of ASME Turbo Expo*, 2008.
[11] Dhondt, G. *The finite element method for three-dimensional thermo mechanical applications.* Münich, Germany: ISBN 0- 470-85752-8, 2004.
[12] Amiet, R. K. "Acoustic radiation from an airfoil in turbulent stream." *Sound and Vib.*, 1975: 407-420.
[13] Reboul, G., Polacsek, C., Lewy, S. & Heib, S. "Ducted-fan broadband noise simulations using unsteady or averaged data." *Inter-noise2008 Conference*, 2008.
[14] Hanson, D., B. "Noise of Counter-Rotation Propellers." 1985: Vol. 22 (7).
[15] Kohlhaas, M., Carolus, T. "Trailing Edge Blowing for Reduction of Rotor-Stator Interaction Noise: Criteria, Design and Measurements." *ISROMAC-14*, 2012.
[16] He, L. "Fourier methods for turbomachinery applications." 2010: 329-341.
[17] Cambier, L., Heib, S., and Plot, S. "The ONERA elsA CFD Software: input from research and feedback from industry Journal of Mechanics & Industry." *Online publication.* 2013.